

**Linearised shift and stretch in DOAS**

S. Beirle et al.

This discussion paper is/has been under review for the journal Atmospheric Measurement Techniques (AMT). Please refer to the corresponding final paper in AMT if available.

# Linearisation of the effects of spectral shift and stretch in DOAS analysis

S. Beirle<sup>1</sup>, H. Sihler<sup>1,2</sup>, and T. Wagner<sup>1</sup>

<sup>1</sup>Max-Planck-Institut für Chemie, Mainz, Germany

<sup>2</sup>Institut für Umweltphysik, Universität Heidelberg, Heidelberg, Germany

Received: 3 October 2012 – Accepted: 13 November 2012 – Published: 21 November 2012

Correspondence to: S. Beirle (steffen.beirle@mpic.de)

Published by Copernicus Publications on behalf of the European Geosciences Union.

Title Page

Abstract

Introduction

Conclusions

References

Tables

Figures

◀

▶

◀

▶

Back

Close

Full Screen / Esc

Printer-friendly Version

Interactive Discussion



## Abstract

Differential Optical Absorption Spectroscopy (DOAS) is a widely used method to quantify atmospheric trace gases from spectroscopic measurements. While DOAS can in principal be described by a linear equation system, usually non-linearities occur, in particular as a consequence of spectral misalignments.

Here we propose to linearise the effects of a spectral shift by including a “shift spectrum”, which is the first term of a Taylor expansion, as pseudo-absorber in the DOAS fit. The effects of a spectral stretch are considered as additional wavelength-dependent shifts.

Solving the DOAS equation system linearly has several advantages: the solution is unique, the algorithm is robust, and it is very fast. The latter might be particularly important for measurements with high data rates, like for upcoming satellite missions.

## 1 Introduction

Differential Optical Absorption Spectroscopy (DOAS) (Platt, 1994) is an established method for the analysis of atmospheric composition. Based on the Beer-Lambert law, and making use of the characteristic absorption features of various trace gases in the UV/vis spectral range, several important trace gases, like ozone or nitrogen dioxide ( $\text{NO}_2$ ), can be quantified. For a comprehensive description of the DOAS method and its application, see e.g. Platt (1994); Platt and Stutz (2008); Richter and Wagner (2011), and references therein.

The DOAS approach can be formulated in terms of optical depth (OD)  $\tau$  as

$$\tau := \ln \frac{I}{I_0} = - \sum s_i \sigma_i + P \quad (1)$$

(compare Richter and Wagner, 2011, Eq. 2.10).  $I$  denotes the measured intensity.  $I_0$  is the initial intensity of the light source (“reference spectrum”).  $\sigma_i$  is the

## Linearised shift and stretch in DOAS

S. Beirle et al.

Title Page

Abstract

Introduction

Conclusions

References

Tables

Figures

◀

▶

◀

▶

Back

Close

Full Screen / Esc

Printer-friendly Version

Interactive Discussion



**Linearised shift and stretch in DOAS**

S. Beirle et al.

[Title Page](#)[Abstract](#)[Introduction](#)[Conclusions](#)[References](#)[Tables](#)[Figures](#)[◀](#)[▶](#)[◀](#)[▶](#)[Back](#)[Close](#)[Full Screen / Esc](#)[Printer-friendly Version](#)[Interactive Discussion](#)

wavelength-dependent absorption cross-section of the  $i$ th relevant trace gas, and  $s_i$  is the respective slant column density (SCD), i.e. the concentration integrated along the effective light path.  $P$  is a closure polynomial which accounts for broad-band wavelength dependencies of Rayleigh or Mie scattering, surface reflectance, etc.

Note that besides molecular absorptions, further phenomena can affect the spectral structures of the OD, as, for instance, the so-called “Ring effect” (Solomon et al., 1987), caused by inelastic Raman scattering. In practice, such spectral structures are often accounted for by introducing additional “pseudo absorbers” like a “Ring spectrum”. Other common pseudo-absorbers are an “undersampling spectrum” to account for the effects of spectral undersampling (Slijkhuis et al., 1999), or the inverse irradiance, to account for an additive stray-light offset (Noxon, 1979). Mathematically, such pseudo-absorbers have the same functionality as the cross-sections in the fitting procedure, while physical meaning and units of the fit coefficients are different.

For measured spectra of  $I$  and  $I_0$ , Eq. (1) results in a system of  $N$  linear equations with  $M$  unknowns, where  $N$  is the number of detector pixels in the considered wavelength range, and  $M$  is the sum of (pseudo-)absorbers and polynomial coefficients. If overdetermined ( $N \gg M$ ), this system can easily be solved by simple Matrix operations, e.g. by calculating the pseudo-inverse, which is mathematically equivalent to a least-squares minimization (Williams, 1990).

However, if spectral misalignments occur, i.e. if the wavelengths assigned to the detector pixels do not match for  $I$ ,  $I_0$ , or the involved cross-sections, the SCDs resulting from a linear algorithm are systematically biased (Stutz and Platt, 1996). Such spectral misalignments could be caused by inaccurate reference cross-sections  $\sigma_i$ , temperature changes of the spectrometer ( $I$ ), instabilities of the light source ( $I_0$ ), etc. Section 2 lists typical shifts for different DOAS applications.

To account for such spectral misalignments, it is common practice to allow for a spectral shift and stretch/squeeze as additional free parameters within the DOAS analysis. This approach can reduce systematic errors significantly, but with these additional parameters, the system is not linear any more. The solution (or simply “fit” hereafter)

requires non-linear least square minimization algorithms, like the iterative Levenberg-Marquardt algorithm (Marquardt, 1963). Compared to the simple and unique solution of the linear equation system, the non-linear fit has several disadvantages:

- It is considerably slower, as it requires the calculation of partial derivatives for all parameters in each iteration step.
- It is not unique and the fit results depend on the predefined termination criteria.
- In a non-linear system, local minima can exist. Consequently, the fit results can depend on the initial values of the state vector, and the fit might even diverge for an offside initial state vector.

The aspect of speed might become particularly relevant for future satellite missions like TROPOMI (Veefkind et al., 2012) with high data rates ( $\sim 12$  GB per orbit, or some hundred spectra per second).

Here we propose a linearisation scheme to account for spectral misalignments (shift and stretch) between  $I$  and  $I_0$ , similar to the approach used by Rozanov et al. (2011).

After a short summary of DOAS applications and their typical spectral misalignments (Sect. 2), we investigate the spectral patterns caused by a shift or stretch by performing a Taylor expansion of  $I$ . In first order, the linear term can be simply added as pseudo-absorber to the DOAS Eq. (1), while maintaining its linearity (Sect. 3). The accuracy and performance of our proposed linearisation are investigated for a standard DOAS application, i.e. the retrieval of  $\text{NO}_2$  in the blue spectral range, in Sect. 4. In Sect. 5, we discuss various aspects of our approach, and sum up our findings in the conclusions.

## 2 DOAS applications and their typical shifts

Here we shortly summarize different DOAS applications insofar as related to this study. For details see e.g. Platt and Stutz (2008).

### Linearised shift and stretch in DOAS

S. Beirle et al.

Title Page

Abstract

Introduction

Conclusions

References

Tables

Figures

◀

▶

◀

▶

Back

Close

Full Screen / Esc

Printer-friendly Version

Interactive Discussion



## 2.1 Active DOAS

For an active DOAS system, an artificial light source, like a xenon arc lamp, or, recently, also a LED, is used. The effects of spectral misalignments depend on the high-frequency structures of the lamp spectrum, which are usually rather small compared to the Fraunhofer lines in solar spectra.

Spectral shifts for active DOAS systems can be caused e.g. by temperature drifts of the spectrometer or by insufficient mode mixing, and can reach values of  $\sim 0.02$  nm. But computational costs are generally not critical for active DOAS measurements, due to the limited data sets. Thus, we focus on passive DOAS applications in this study.

## 2.2 Passive DOAS applications

Passive DOAS set-ups use the sun as light source. Thus, the measured spectra of scattered sunlight are usually dominated by Fraunhofer lines. This allows one to create a calibrated reference frame (i.e. a set of reference spectrum, absorption cross-sections, and pseudo-absorbers, spectrally calibrated and defined on the spectrometer's pixel grid) by the following steps:

- A reference spectrum  $I_0$  (measured by the spectrometer) is chosen.
- $I_0$  is calibrated (i.e. the wavelength-pixel allocation is determined) by means of a well-calibrated, high-resolution solar spectrum (e.g. Chance and Kurucz, 2010), making use of the dominant Fraunhofer lines. The instrument function of the spectrometer either has to be known or can be determined during the calibration.
- According to this calibration, laboratory absorption cross-sections are convolved and interpolated on the spectrometer's pixel grid.
- Pseudo-absorbers, in particular the Ring spectrum and the inverse ( $\frac{1}{I_0}$ ) in order to account for stray light, are derived from  $I_0$ .

### Linearised shift and stretch in DOAS

S. Beirle et al.

Title Page

Abstract

Introduction

Conclusions

References

Tables

Figures

◀

▶

◀

▶

Back

Close

Full Screen / Esc

Printer-friendly Version

Interactive Discussion



These steps can be easily performed using DOAS software platforms as DOASIS (Kraus, 2005) or WINDOAS (Fayt and van Roozendael, 2001).

### 2.2.1 Zenith sky DOAS

Zenith-sky measurements from ground-based spectrometers allow to analyse time series of (mostly stratospheric) trace gases. The solar reference is typically taken from noon-time measurements. (Note that this is not a real solar spectrum, but is already affected by atmospheric absorption. The fitted SCDs are thus differential SCDs with respect to " $I_0$ "). If  $I_0$  is used for a time-series of several days to months, typical shifts are of the order of 0.001 up to 0.01 nm, respectively. If daily solar references are used, typical shifts are generally  $< 0.002$  nm.

### 2.2.2 MAX-DOAS

Multi-Axis (MAX) DOAS measurements provide additional information on surface-near vertical trace gas profiles (e.g. Hönninger et al., 2004; Wagner et al., 2011). Usually a zenith sky measurement is used as solar reference. If  $I_0$  is applied to a time-series of several days to months, typical shifts are of the order of 0.002 to 0.01 nm, respectively. If daily solar references are used, or even a separate  $I_0$  for each elevation angle sequence, shifts are generally  $< 0.002$  nm.

### 2.2.3 Satellite observations

Several spectrometers with moderate spectral resolution are in orbit, e.g. GOME, SCIAMACHY, GOME-2, or OMI, providing global information on various atmospheric trace gases (e.g. Wagner et al., 2008; Martin, 2008). Direct solar measurements are taken by these spectrometers typically once per day. Due to the high speed of the satellites, spectral misalignments are dominated by the Doppler-effect (Slijkhuis et al., 1999), which causes shifts of about 0.01 nm for  $\lambda = 440$  nm. Thus, for satellite retrievals, a modified reference set should be created (by shifting  $I_0$ , cross-sections

## Linearised shift and stretch in DOAS

S. Beirle et al.

Title Page

Abstract

Introduction

Conclusions

References

Tables

Figures

◀

▶

◀

▶

Back

Close

Full Screen / Esc

Printer-friendly Version

Interactive Discussion



and pseudo-absorbers accordingly) which already accounts for the Doppler shift (see Sect. 5.2). The remaining shift variations relative to this overall offset are below 0.002 nm.

### 3 Method

5 Based on Eq. (1), the DOAS fit is equivalent to a simple linear equation system, as long as spectral alignment is given. Here, we investigate the spectral structures caused by a spectral misalignment between  $I$  and  $I_0$ , and derive pseudo-absorbers which account for these effects in first (linear) order. A potential misalignment of a cross-section  $\sigma_i$  can not be linearised in analogous form, as shown in Appendix A.

#### 10 3.1 Spectral shift

To investigate the effects of a spectral shift, i.e. a simple offset of  $\Delta\lambda$  in the wavelength-pixel allocation between  $I$  and  $I_0$ , we reformulate Eq. (1) as

$$\ln(I) - \ln(I_0) = \sum s_i \sigma_i + P. \quad (2)$$

15 If the cross-sections  $\sigma_i$  and  $I_0$  are spectrally calibrated on the detector's grid (see Sect. 2), but  $I$  is shifted by  $\Delta\lambda$ , artificial spectral structures are created which can be approximated by a Taylor expansion:

$$\begin{aligned} \ln(I(\lambda + \Delta\lambda)) &= \ln(I(\lambda)) + \frac{d}{d\lambda} \ln(I(\lambda)) \Delta\lambda + \mathcal{O}(2) \\ &= \ln(I(\lambda)) + \frac{1}{I(\lambda)} \frac{d}{d\lambda} I(\lambda) \Delta\lambda + \mathcal{O}(2) \\ &= \ln(I(\lambda)) + \frac{I'(\lambda)}{I(\lambda)} \Delta\lambda + \mathcal{O}(2) \\ &\approx \ln(I(\lambda)) + A_{\text{Shift}} \Delta\lambda \end{aligned} \quad (3)$$

20

## Linearised shift and stretch in DOAS

S. Beirle et al.

Title Page

Abstract

Introduction

Conclusions

References

Tables

Figures

◀

▶

◀

▶

Back

Close

Full Screen / Esc

Printer-friendly Version

Interactive Discussion



$\mathcal{O}(2)$  denotes second and higher order terms. The errors introduced by the linearisation are quantified by the second term of the Taylor expansion below.

A spectral shift  $\Delta\lambda$  of  $I$  thus causes, in first order, a spectral structure which is proportional to

$$A_{\text{Shift}} := \frac{I'(\lambda)}{I(\lambda)}. \quad (4)$$

This “shift-spectrum”  $A_{\text{Shift}}$ , i.e. the derivative of  $\ln(I(\lambda))$ , can now be included as pseudo-absorber to the equation system, while maintaining its linearity. The respective fit coefficient directly yields the shift  $\Delta\lambda$ . A similar approach was used in Rozanov et al. (2011, Eq. 20) for the retrieval of BrO profiles from SCIAMACHY limb measurements.

We illustrate the effect of a spectral shift on  $I$  for a simple Gaussian absorption band at  $\lambda_0$ :

$$\tau_{\text{SB}} = ae^{-\frac{\lambda^2}{2\zeta^2}}, \quad (5)$$

where the subscript “SB” stands for “single band”.  $a$  and  $\zeta$  are the band depth and width, respectively, and  $\bar{\lambda}$  is the wavelength relative to the band center:

$$\bar{\lambda} := \lambda - \lambda_0. \quad (6)$$

For simplicity, we assume a perfect white light source  $I_0 \equiv 1$ . It is thus

$$I_{\text{SB}} = e^{-\tau_{\text{SB}}} = e^{-ae^{-\frac{\lambda^2}{2\zeta^2}}}. \quad (7)$$

Figure 1a displays  $I_{\text{SB}}$  (black) for  $a = 0.2$  and  $\zeta = 5$  pixel, and  $I_{\text{SB}}$  shifted by 1 pixel (blue). Figure 1b shows, in blue, the spectral structure (in terms of OD) caused by the shift, calculated as  $\ln(I_{\text{shifted}}) - \ln(I)$ . In green, the respective structure resulting from the

Linearised shift and stretch in DOAS

S. Beirle et al.

Title Page

Abstract

Introduction

Conclusions

References

Tables

Figures

◀

▶

◀

▶

Back

Close

Full Screen / Esc

Printer-friendly Version

Interactive Discussion





linearisation in Eq. (3) is shown, i.e. the pseudo-absorber  $A_{\text{Shift}}$  as defined in Eq. (4), scaled by the applied shift.

For  $I_{\text{SB}}$ , the shift-spectrum can directly be calculated:

$$A_{\text{Shift}} = \frac{I'_{\text{SB}}}{I_{\text{SB}}} = -\tau'_{\text{SB}} = \frac{\bar{\lambda}}{\zeta^2} \tau_{\text{SB}}. \quad (8)$$

5 It has its maximum/minimum at  $\bar{\lambda} = \pm\zeta$ , where  $A_{\text{Shift}}$  is  $\pm \frac{a}{\zeta} e^{-\frac{1}{2}}$  (compare Fig. 1b). To first order, a spectral shift of  $\Delta\lambda$  thus causes spectral structures (peak-to-peak OD) of  $(\max(A_{\text{Shift}}) - \min(A_{\text{Shift}})) \times \Delta\lambda$ :

$$\mathcal{O}(1) = 1.2 \times a \frac{\Delta\lambda}{\zeta}, \quad (9)$$

10 i.e. they are proportional to the shift itself, to the depth of the absorption lines, and reciprocal to the width of the absorption lines. In other words, deep narrow absorption lines are most critical for a spectral misalignment. For the sample values ( $a = 0.2$ ,  $\zeta = 5$  and  $\Delta\lambda = 1$ ), Eq. (9) yields a peak-to-peak OD of 5%, in agreement with Fig. 1.

15 It can be seen that  $A_{\text{Shift}}$  reproduces well the spectral structures caused by the shift. The remaining errors, i.e. the difference of the curves in Fig. 1b, are caused by the neglect of higher orders in Eq. (3). The second order term of the Taylor expansion is

$$\mathcal{O}(2) = \frac{1}{2} \frac{d^2}{d\lambda^2} \ln(I) \Delta\lambda^2 = \frac{1}{2} \frac{d}{d\lambda} \frac{I'}{I} \Delta\lambda^2 = \frac{1}{2} \frac{I''/I - I'I''}{I^2} \Delta\lambda^2. \quad (10)$$

For  $I_{\text{SB}}$ , it is

$$\frac{1}{2} \frac{d^2}{d\lambda^2} \ln(I) \Delta\lambda^2 = \frac{1}{2} \frac{d}{d\lambda} (-\tau'_{\text{SB}}) \Delta\lambda^2 = \frac{1}{2} \frac{d}{d\lambda} \left( \frac{\bar{\lambda}}{\zeta^2} \tau_{\text{SB}} \right) \Delta\lambda^2 = \frac{1}{2} \frac{\tau_{\text{SB}}}{\zeta^2} \left( 1 - \frac{\bar{\lambda}^2}{\zeta^2} \right) \Delta\lambda^2. \quad (11)$$

This function is maximum at  $\bar{\lambda} = 0$  and minimum at  $\bar{\lambda} = \pm\sqrt{3}\zeta$ . Thus (Eq. 5), the peak-to-peak distance is  $\frac{1}{2}\frac{a}{\zeta^2}(1+2e^{-\frac{3}{2}})\Delta\lambda^2$ . The second-order peak to peak effects of a spectral shift are thus

$$\mathcal{O}(2) = 0.7 \times a \frac{\Delta\lambda^2}{\zeta^2}. \quad (12)$$

5 For the example shown in Fig. 1, this is  $\approx 0.6\%$ , i.e. about one order of magnitude lower than the first-order term accounted for by  $A_{\text{Shift}}$ . These orders of magnitudes as derived for a general absorption band (Eqs. 9 and 12) also proved to be meaningful for complex spectra (see Sect. 4).

10 The third order term is proportional to  $\frac{\Delta\lambda^3}{\zeta^3}$ , i.e. negligible for typical shifts (see Sect. 2).

### 3.2 Spectral stretch

In addition to a spectral shift, the wavelength-pixel allocations might also be linearly transformed by a factor  $q$ , i.e. stretched ( $q > 1$ ) or squeezed ( $q < 1$ ) relative to each other (below we use the generic term “stretch” in a general meaning for both  $q > 1$  and  
15  $q < 1$ ). Here we define the stretch  $q$  with respect to the central wavelength of the fitting window  $\lambda_0$  as:

$$\lambda' = q(\lambda - \lambda_0) + \lambda_0 + \Delta\lambda. \quad (13)$$

By this definition of the stretch-parameter  $q$ , the stretch does not affect the central wavelength of the fitting window, i.e. overall, it does not introduce an additional shift.  
20 However, locally, such a stretch is equivalent to a (wavelength dependent) shift: At a given wavelength, the spectral displacement  $D$  can be expressed as

$$\begin{aligned} D &:= \lambda' - \lambda = q(\lambda - \lambda_0) + \lambda_0 + \Delta\lambda - \lambda \\ &= (q - 1)(\lambda - \lambda_0) + \Delta\lambda, \end{aligned} \quad (14)$$

## Linearised shift and stretch in DOAS

S. Beirle et al.

Title Page

Abstract

Introduction

Conclusions

References

Tables

Figures

◀

▶

◀

▶

Back

Close

Full Screen / Esc

Printer-friendly Version

Interactive Discussion



i.e. locally, a shift of  $(q - 1)(\lambda - \lambda_0)$  is added to the overall shift  $\Delta\lambda$ . Similarly to  $\Delta\lambda$ , this additional shift causes, in first order, spectral structures of  $A_{\text{Shift}}(\lambda - \lambda_0)(q - 1)$ . Thus, a spectral stretch can be accounted for by adding the pseudo-absorber (“stretch-spectrum”)

$$A_{\text{Stretch}} := A_{\text{Shift}}(\lambda - \lambda_0) \quad (15)$$

to the linear equation system. The respective fit coefficient is  $(q - 1)$ . Figure 2 shows the effects of a spectral stretch and the stretch spectrum analogously to Fig. 1.

In principle, also higher orders of spectral misalignments (quadratic terms etc.) could be considered as well in an analogous way, i.e. by defining the pseudo-absorber of  $n$ th order as  $A_n := A_{\text{Shift}}(\lambda - \lambda_0)^n$ . Here, we focus on the effects of shift ( $\hat{=A}_0$ ) and stretch ( $\hat{=A}_1$ ).

As a stretch can be regarded as wavelength dependent shift, the errors of the linearisation can be evaluated similar to Sect. 3.1 according to the maximum pixel displacement caused by the stretch.

### 3.3 Pseudo-absorbers for $I_0$

The shift-spectrum was defined in Eq. (4) based on a Taylor expansion of a shifted radiance  $I$ . Here, we define a similar shift-spectrum based on  $I_0$ :

$$B_{\text{Shift}} := \frac{I'_0}{I_0}. \quad (16)$$

The respective stretch-spectrum is defined analogously to Eq. (15):

$$B_{\text{Stretch}} := B_{\text{Shift}}(\lambda - \lambda_0). \quad (17)$$

Deriving the pseudo absorbers from  $I_0$  instead of  $I$  may seem illogical, as  $I_0$  is spectrally calibrated against a high-resolution, well-calibrated solar reference, and thus not

**Linearised shift and stretch in DOAS**

S. Beirle et al.

Title Page

Abstract

Introduction

Conclusions

References

Tables

Figures

◀

▶

◀

▶

Back

Close

Full Screen / Esc

Printer-friendly Version

Interactive Discussion



**Linearised shift and stretch in DOAS**

S. Beirle et al.

[Title Page](#)[Abstract](#)[Introduction](#)[Conclusions](#)[References](#)[Tables](#)[Figures](#)[⏪](#)[⏩](#)[◀](#)[▶](#)[Back](#)[Close](#)[Full Screen / Esc](#)[Printer-friendly Version](#)[Interactive Discussion](#)

subject to further shifts. But if the difference between  $B_{\text{Shift/Stretch}}$  and  $A_{\text{Shift/Stretch}}$  is negligible, which is the case if the spectral structures of both  $I$  and  $I_0$  are dominated by the strong Fraunhofer lines and the OD of atmospheric absorbers  $\tau$  is low, this approach has high practical relevance, as it allows one to create a complete, consistent reference frame just based on  $I_0$ , which can be applied for a sequence (e.g. one satellite orbit) of radiance measurements. In contrast, the exact calculation of the pseudo-absorbers based on  $I$  would imply the calculation of derivatives for each measured spectrum, before the linear fit can be performed.

Both approaches are investigated in the next section for a concrete example, and the applicability of  $B_{\text{Shift/Stretch}}$  instead of  $A_{\text{Shift/Stretch}}$  is discussed further in Sect. 5.3.

## 4 Sample application: NO<sub>2</sub> retrieval

In this section, we analyse the accuracy and performance of the proposed implementation of spectral shift and stretch in the DOAS analysis by pseudo-absorbers, in comparison to the “classical” non-linear DOAS, for a standard DOAS application, i.e. the fit of NO<sub>2</sub> in the blue spectral range.

### 4.1 Setup

To investigate the accuracy of the linear versus non-linear DOAS fit, we model synthetic spectra, which allows us to compare the fit results to the a-priori “truth”.

We consider a detector with a spectral resolution of 0.55 nm FWHM and a spectral sampling of 0.2 nm, as for TROPOMI in the blue spectral range (Veefkind et al., 2012). Starting with a high-resolution solar irradiation spectrum (Chance and Kurucz, 2010),  $I_0$  is determined in detector resolution by assuming a Gaussian slit function. The radiance  $I$  is calculated by considering rotational Raman scattering and the absorption of NO<sub>2</sub>, corresponding to optical depths (peak-to-peak) of 5 % and 1 %, respectively, plus a broad-band absorption. Note that the dependency of the resulting fit bias of the NO<sub>2</sub>

SCD on shift and stretch has been found to be not dependent on the a-priori  $\text{NO}_2$  SCD in the simulation.

$I$  is then manipulated by a variety of spectral displacements. Table 1 lists the applied shift and stretch parameters. The fit accuracy is analysed for “ideal” spectra, as well as for spectra where a Gaussian random noise with a standard deviation of 0.015 % of the maximum radiance is added to  $I$ . This noise level corresponds to residues of about 0.1 % peak-to-peak.

The pseudo-absorbers  $A_{\text{Shift}}$  and  $A_{\text{Stretch}}$  are determined from  $I$  according to Eqs. (4) and (15), and  $B_{\text{Shift}}$  and  $B_{\text{Stretch}}$  from  $I_0$  according to Eqs. (16) and (17), respectively. Note that the calculation of the discrete derivatives  $I'$  or  $I'_0$  has to be done properly, as a simple difference quotient was found to be not accurate enough. This aspect is discussed in Appendix B.

Finally, the shifted and stretched radiances are analysed by linear (with and without the proposed pseudo-absorbers) and non-linear DOAS at 430–450 nm. For this, the commercial software MATLAB, as well as DOASIS (Kraus, 2005), have been used.

## 4.2 Results

Figure 3 illustrates the effect of the shift and the accuracy of the fit exemplarily for a shift of  $\Delta\lambda = 0.02$  nm, i.e. a tenth of a pixel. The figure displays only half of the fitting window to zoom in the small horizontal displacements.

Figure 3a displays  $I_0$  (black) and the original (grey) and shifted (blue) radiances, which can be hardly discriminated. In Fig. 3b, the respective OD is shown for  $I$  (grey, revealing the combined structures caused by the applied Ring effect and  $\text{NO}_2$  absorption), and  $I_{\text{shifted}}$  (blue, revealing additional spectral structures due to the shift  $\Delta\lambda$ ).

In Fig. 3c, the difference of both OD (“true” and “shifted”) from Fig. 3b are displayed in blue, analogously to the simple example shown in Fig. 1b, showing spectral structures of about 3.5 % peak-to-peak caused by the spectral mismatch. Note that this structure is very similar to the fit residue of the linear fit without shift- and stretch-spectra (not shown), but not identical, as the fit tries to “explain” part of the shift structures by the

## Linearised shift and stretch in DOAS

S. Beirle et al.

Title Page

Abstract

Introduction

Conclusions

References

Tables

Figures

◀

▶

◀

▶

Back

Close

Full Screen / Esc

Printer-friendly Version

Interactive Discussion



considered (pseudo-) absorbers Ring and NO<sub>2</sub>. The shift spectra  $A_{\text{Shift}}$  and  $B_{\text{Shift}}$ , as defined in Eqs. (4) and (16), scaled by the applied shift, are shown in green/orange, respectively. They both reproduce well the spectral structures caused by the spectral misalignment.

Figure 3d displays the residue of the linear fit including  $A_{\text{Shift}}$  and  $A_{\text{Stretch}}$  as pseudo-absorbers in green, and  $B_{\text{Shift/Stretch}}$  in orange. The remaining remaining residue is about 0.11 % (*A*) and 0.15 % (*B*) peak-to-peak, i.e. more than one order of magnitude lower than for the simple linear fit. Note that the residue for the non-linear fit, shown in red, depends on the settings of the Levenberg-Marquardt-Algorithm, in particular on the allowed number of iterations and the predefined termination criteria.

If we estimate the shift effects from Eqs. (9) and (12), we expect (for  $a \approx 0.4$ ,  $\zeta \approx 0.3\text{nm}$ , and  $\Delta\lambda = 0.02\text{nm}$ ) spectral structures of the order of 3.2 %, in agreement with Fig. 3c, and unresolved residues of about 0.12 %, in good agreement with Fig. 3d. I.e. the estimates derived for a single band can also be used to estimate the order of magnitude for a complex multi-band spectrum.

In Fig. 4, the fitted shift and stretch parameters are compared to the actually applied values. Note that for the linear fit (green), the shift and stretch parameters are simply the fit coefficients for the pseudo-absorbers  $A_{\text{Shift}}$  and  $A_{\text{Stretch}}$ , i.e.  $\Delta\lambda$  and  $q-1$ , respectively, while  $l$  is not changed. In contrast, for the non-linear fit (red), a real shift/stretch is performed to  $l$  in each iteration step. It can be seen that both fits actually reproduce the applied shifts/stretches with high accuracy. For the non-linear and linear fit, relative deviations between fitted and true shift  $\Delta\lambda$  are less than 0.4 % and 3 %, respectively, for displacements  $< 0.03\text{nm}$ . For a linear fit including  $B_{\text{Shift}}$  (not shown), the relative deviations are slightly higher (up to 13 %).

Now we investigate the resulting SCDs for the variety of shifts and stretches listed in Table 1. For each shift/stretch combination, we define the “maximum displacement” as the maximum of all detector pixel displacements  $D$  within the fit window, in order to have a single abscissa. For instance, for a shift of 0.1 pixel, i.e. 0.02 nm, and a stretch

**Linearised shift and stretch in DOAS**

S. Beirle et al.

Title Page

Abstract

Introduction

Conclusions

References

Tables

Figures

◀

▶

◀

▶

Back

Close

Full Screen / Esc

Printer-friendly Version

Interactive Discussion



of 1.01, the spectral displacement, according to Eq. (14), is maximum at the right edge of the fitting window, where it is  $(q - 1)(\lambda - \lambda_0) + \Delta\lambda = 0.12$  nm.

Figure 5a shows the resulting fit residues for all combinations of shift and stretch, up to a maximum displacement of 0.03 nm, on a log-log-scale. The straight lines indicate the expected first (purple) and second (green) order estimate according to Eqs. (9) and (12) for  $a = 0.4$  and  $\zeta = 0.3$  nm. The absolute deviations of the fitted NO<sub>2</sub> SCDs from the true (a-priori) value are shown in Fig. 5b. In addition, values for a shift of 0.002 nm are listed in Table 2.

Purple dots show the results for the simple linear fit ignoring shift and stretch, revealing residues according to the first order estimate. For a displacement of 0.002 nm (i.e. 1 % of a pixel), residues are 0.33 %. The respective NO<sub>2</sub> SCDs are biased by  $3.2 \times 10^{14}$  molecules cm<sup>-2</sup>, which is of the order of fit uncertainties of NO<sub>2</sub> SCDs from satellite retrievals (Boersma et al., 2004). Compared to this, the fit results are significantly improved if shift and stretch are included as pseudo-absorbers to the linear fit (green): both the residue and the NO<sub>2</sub> bias are generally reduced by more than two orders of magnitude. At a displacement of 0.002 nm, the residue and NO<sub>2</sub> bias are now only about  $10^{-5}$  and  $10^{12}$  molecules cm<sup>-2</sup>, respectively, which is negligible, and quite close to the results of the non-linear fit. For pseudo-absorbers derived from  $I_0$  (orange), the results are slightly worse ( $5 \times 10^{-5}$  residue and  $5 \times 10^{12}$  molecules cm<sup>-2</sup> bias), but still far better than those of a linear fit without pseudo-absorbers. For smaller displacements, the bias decreases approximately quadratically (according to Eq. 12) for  $A$ , as expected (as the quadratic term is neglected in Eq. 3). For  $B$ , the decrease is slower ( $\approx$ linear) due to the additional approximation, i.e. the neglect of atmospheric trace gas absorptions in the calculation of the pseudo-absorbers (compare Eq. 18).

Figure 6 shows the respective fit results for the simulated spectra with additional noise. 300 runs have been performed, and the resulting residues and biases are averaged. Table 2 shows mean and standard deviation for a shift of 0.002 nm.

The noise truncates the fit residues (peak-to-peak) of all fits to  $\gtrsim 0.1$  %. Still, the linear fit without shift/stretch performs poorly, while the other methods (linear with pseudo

**Linearised shift and stretch in DOAS**

S. Beirle et al.

Title Page

Abstract

Introduction

Conclusions

References

Tables

Figures

◀

▶

◀

▶

Back

Close

Full Screen / Esc

Printer-friendly Version

Interactive Discussion



absorbers and non-linear) show lower residues by a factor of about 3 for the typical shifts of 0.002 nm for passive DOAS-applications.

The bias is quite low on average for all fits except the simple linear case. But the standard deviation of the bias caused by the noise is about  $1.6 \times 10^{14}$  molecules  $\text{cm}^{-2}$  for a shift of 0.002 nm.

For the noisy radiances, the non-linear fit shows neither lower residues nor lower  $\text{NO}_2$  biases compared to the linear fit with pseudo-absorbers. Thus, for practical applications, noise levels of  $> 0.015\%$  and shifts  $< 0.002$  nm, there is no benefit from the non-linear fit at all, and the pseudo-absorbers can be derived from  $I_0$  instead of  $I$ , at least for the analysis of  $\text{NO}_2$  (see also the Discussions in Sect. 5).

### 4.3 Computation time

The fits have been performed on a Windows XP system with an Intel Core 2 Duo CPU T9300 at a frequency of 2.50 GHz. The synthetic spectra have been analysed using DOASIS (Kraus, 2005) as well as MATLAB. For the linear fit, the results from both implementations are identical. For the non-linear fits, small (but insignificant) deviations occur due to the different implementations and termination criteria. The computation times for a single fit (without noise) are compared in Table 3. For the spectra affected by gaussian noise, computation times are about 2 to 3 times higher. The non-linear fit is faster by a factor of 10 for the DOASIS implementation compared to MATLAB, as could be expected, since DOASIS is optimized for this method, and the mathematical operations are processed by pre-compiled, executable code, while MATLAB is a script language. But interestingly, for the linear fit, MATLAB performs better than DOASIS; this is probably due to the fact that MATLAB is optimized for linear matrix operations, and DOASIS seems to step into the iterative Levenberg-Marquardt algorithm, even though the non-linear parameters, namely shift and stretch, are fixed. We conclude that DOASIS yields realistic numbers ( $4 \times 10^{-3}$  s per fit) for the computation time of the non-linear fit, while for the linear fit, the results from MATLAB gives an upper limit of what can be achieved for linear algorithms ( $4 \times 10^{-5}$  s per fit). I.e. the linear fit is

## Linearised shift and stretch in DOAS

S. Beirle et al.

Title Page

Abstract

Introduction

Conclusions

References

Tables

Figures

◀

▶

◀

▶

Back

Close

Full Screen / Esc

Printer-friendly Version

Interactive Discussion





at least faster by two orders of magnitude. Further acceleration of the linear fit can possibly be gained using optimized code on GPUs (Graphic Processor Units), which are particularly suited for linear operations.

If we apply these numbers to one orbit of TROPOMI with about one million spectra (P. Veefkind, personal communication), the computation time would be about 4000 s (> one hour) for the non-linear fit, but only 40 s for the linear fit, without consideration of input/output operations.

## 5 Discussion

The proposed treatment of shift- and stretch effects as pseudo-absorbers allows one to solve the DOAS equation system linearly. For typical noise levels, the fit accuracy almost equals that of a non-linear fit. The linearisation significantly speeds up the DOAS fit, which is particularly relevant for satellite measurements. Here we discuss further advantages, aspects, and restrictions of our approach.

### 5.1 Quick assessment of the spectral calibration

Apart from fitting trace gas SCDs, the pseudo-absorbers  $A_{\text{Shift/Stretch}}$  allow the quick assessment of the spectral calibration of a given spectrum: the respective fit parameters directly yield the spectral shift  $\Delta\lambda$  and stretch ( $q - 1$ ). Thus, e.g. the mean spectral shift of satellite measurements can quickly be determined (Sect. 5.2), or the need for accounting for a stretch can be easily evaluated.

### 5.2 Pre-shifted set-up

For satellite measurements, the Doppler-effect causes a general shift on top of possible other, generally smaller spectral displacements. Note that for the  $\text{NO}_2$  fit discussed in Sect. 4, the linear fit works as well as the non-linear fit for noisy radiances, even for shifts as large as 0.01 nm. In cases, however, where the Doppler shift effects become

## Linearised shift and stretch in DOAS

S. Beirle et al.

Title Page

Abstract

Introduction

Conclusions

References

Tables

Figures

◀

▶

◀

▶

Back

Close

Full Screen / Esc

Printer-friendly Version

Interactive Discussion



too large to be linearised, we propose to create a pre-shifted set of reference spectrum and cross-sections, by applying a mean shift  $\Delta\lambda_0$ . With these pre-shifted  $I_0^*$  and  $\sigma_i^*$ , a linear fit can be performed, where the resulting shifts are defined relative to  $\Delta\lambda_0$ .

### 5.3 Pseudo-absorbers derived from $I_0$

5 As mentioned in Sect. 3.3, calculating the pseudo absorbers from  $I'_0/I_0$  instead of  $I'/I$  has high practical relevance for satellite retrievals:  $I'_0/I_0$  needs to be calculated only once per reference spectrum, i.e. once per day for satellite measurements, and enables one to use one consistent reference frame for the complete day.

10 For passive DOAS applications, both  $I$  and  $I_0$  are usually dominated by the strong Fraunhofer lines. Thus,  $B_{\text{Shift}}$  is generally similar to  $A_{\text{Shift}}$ ; they differ by the derivative of the OD:

$$B_{\text{Shift}} - A_{\text{Shift}} = \tau' \quad (18)$$

(compare Eq. 1).

15 For  $\tau$  with a peak-to-peak OD of  $b$ , the order of magnitude of  $\tau'$  is about  $b/\zeta$ . If, in addition, the spectral structures of the OD are dominated by the Ring effect, the peak width  $\zeta$  will be similar to that of  $I$ . Consequently, the relative deviation between  $A_{\text{Shift}}$  and  $B_{\text{Shift}}$  is about  $b/a$ , i.e. the ratio of the order of magnitude of  $\tau$  and the depth of the Fraunhofer lines. Note that the impact on the fit results is even less, as  $B_{\text{Shift}}$  can be scaled by the fit. Therefore only different patterns of  $B_{\text{Shift}}$  compared to  $A_{\text{Shift}}$  can cause an additional SCD bias.

20 For the analysis of  $\text{NO}_2$ , the errors induced by  $B_{\text{Shift}}/\text{Stretch}$  have been found to be generally negligible (Fig. 6). However, this is probably different for DOAS evaluations for trace gases absorbing in the UV, if the OD is dominated by strong ozone absorption bands. In such a case, the pseudo-absorbers  $A$  might have to be used, which implies that the derivative of  $I$  has to be calculated for each individual measured spectrum. This reduces the acceleration due to the linearisation by about 20 %, if the derivative is calculated according to Eq. (B3) (see Appendix B).

## Linearised shift and stretch in DOAS

S. Beirle et al.

Title Page

Abstract

Introduction

Conclusions

References

Tables

Figures

◀

▶

◀

▶

Back

Close

Full Screen / Esc

Printer-friendly Version

Interactive Discussion



## 5.4 Missing pixels

An additional advantage of the proposed implementation of spectral misalignments by pseudo-absorbers derived from  $I_0$  instead of  $I$  is the evaluation of radiance measurements  $I$  containing gaps (e.g. due to dead detector pixels); such gaps are problematic for the non-linear fit, as shifting  $I$  involves interpolation, and one missing pixel thus affects (i.e. removes) its neighbours as well. In contrast, for the linear fit, the dead pixels can just be skipped for  $I$ ,  $I_0$ ,  $\sigma$ , and the pseudo-absorbers likewise, and the effect of a potential shift is still accounted for appropriately by the pseudo-absorbers.

In the case of gaps in  $I_0$ , however, these have to be filled in first (e.g. by fitting another solar reference without gaps plus a polynomial), before the derivative  $I'_0$  can be calculated.

## 5.5 Initialization of the non-linear fit

Even if a non-linear DOAS analysis is unavoidable for a given set-up, e.g. due to large shifts or other effects causing non-linearities, the linear fit could still be applied for the calculation of the initial state vector. The subsequent non-linear fit benefits from accurate initial values for SCDs and particularly shift and stretch, and will be more robust and faster. For instance, for a shift of 0.002 nm, the non-linear fit becomes 30 % faster if initialized with the linear fit results including shift- and stretch-spectra.

## 6 Conclusions

Spectral misalignments cause biases in a DOAS analysis and can generally not be neglected. As a consequence, non-linear minimization algorithms are applied in state-of-the-art DOAS analyses, which are far slower than linear algorithms.

### Linearised shift and stretch in DOAS

S. Beirle et al.

Title Page

Abstract

Introduction

Conclusions

References

Tables

Figures

◀

▶

◀

▶

Back

Close

Full Screen / Esc

Printer-friendly Version

Interactive Discussion



We propose to linearise the effects of spectral shifts by the first-order term of a Taylor expansion and introduce a “shift-spectrum”

$$A_{\text{Shift}} := \frac{I'(\lambda)}{I(\lambda)}$$

as pseudo-absorber (compare Rozanov et al., 2011).

5 Spectral stretches can be considered as well by a “stretch-spectrum”

$$A_{\text{Stretch}} := A_{\text{Shift}}(\lambda - \lambda_0),$$

as they can be regarded as additional wavelength-dependent shifts.

10 With these pseudo-absorbers, the DOAS-analysis can be performed linearly, reducing the computational costs by at least 2 orders of magnitude. This is particularly relevant for satellite measurements with high data rates.

Full advantage of the linearisation can be gained if the pseudo-absorbers can be calculated based on  $I_0$ , as they have to be derived only once per reference spectrum instead of once per measurement:

$$B_{\text{Shift}} := \frac{I'_0(\lambda)}{I_0(\lambda)}$$

$$15 B_{\text{Stretch}} := B_{\text{Shift}}(\lambda - \lambda_0).$$

For small absorbers like  $\text{NO}_2$ , this is generally applicable. For strong absorbers like  $\text{O}_3$  in the  $\text{SO}_2$  fit, the pseudo-absorbers might have to be calculated for each radiance spectrum, reducing the speed of the linear fit by about 20%.

The error due to the linearisation, in terms of OD, is

$$20 0.7 \times a \frac{\Delta\lambda^2}{\zeta^2},$$

where  $a$  and  $\zeta$  are the band depths and widths of  $I$ , respectively. For typical shifts  $< 0.002\text{nm}$ , this error ( $\approx 10^{-5}$  in terms of OD) is below typical noise levels.

## Linearised shift and stretch in DOAS

S. Beirle et al.

Title Page

Abstract

Introduction

Conclusions

References

Tables

Figures

◀

▶

◀

▶

Back

Close

Full Screen / Esc

Printer-friendly Version

Interactive Discussion



Even if a non-linear fit is unavoidable (for larger shifts or other non-linear effects), the linear fit can still yield a quick assessment of the spectral calibration of  $I$  and an accurate initial state vector for shift and stretch in the non-linear fit.

## Appendix A

### 5 Spectral misalignments of a cross-section

A cross-section included in a DOAS analysis might be affected by an imperfect spectral calibration as well. Note, however, that there is a basic mathematical difference between intensities and cross-sections in Eq. (1), as the cross-sections are scaled by the SCD during the fit.

10 In general, the spectral structures resulting from a shift in  $\sigma$  could be estimated by a Taylor expansion of  $\sigma$  as well:

$$\begin{aligned}\sigma(\lambda + \Delta\lambda) &= \sigma(\lambda) + \frac{d}{d\lambda}\sigma(\lambda)\Delta\lambda + \mathcal{O}(2) \\ &\approx \sigma(\lambda) + A_{\text{Shift}}^{\sigma}\Delta\lambda\end{aligned}\quad (\text{A1})$$

15 with the pseudo-absorber

$$A_{\text{Shift}}^{\sigma} := \sigma' = \frac{d}{d\lambda}\sigma. \quad (\text{A2})$$

However, the relevant respective structure in OD would be  $A_{\text{Shift}}^{\sigma} \times \Delta\lambda \times s$ . I.e. the fit coefficient  $s$  would appear twice, as factor for both  $\sigma$  and  $\sigma'$ . As  $\sigma'$  has also to be scaled by the shift  $\Delta\lambda$  as free fit parameter, the problem is not linear any more.

20 Figure A1 show the results for a linear fit including  $A_{\text{Shift}}^{\sigma}$  (i.e. ignoring that the problem is not really linear) for the example of a synthetic spectrum with Ring effect (5 % OD) and  $\text{NO}_2$  absorption (5 % OD), where the  $\text{NO}_2$  cross-section is shifted and stretched.

## Linearised shift and stretch in DOAS

S. Beirle et al.

Title Page

Abstract

Introduction

Conclusions

References

Tables

Figures

◀

▶

◀

▶

Back

Close

Full Screen / Esc

Printer-friendly Version

Interactive Discussion



As can be seen, the applied shifts and stretches can not be reproduced by the linear fit due to the remaining non-linearity. The fit accuracy for NO<sub>2</sub> is not much better than that of a simple linear fit ignoring shift effects completely.

Fortunately, spectral shifts of  $\sigma$  do not have a high relevance in most DOAS applications, as cross-sections can generally be measured in laboratory with high accuracy. Additionally, a shift could only significantly affect the DOAS analysis if the respective absorber has a high OD of several percent and narrow absorption lines. Thus, normally, spectral shifts of cross-sections can be neglected. But in the case of an analysis where spectral shifts of  $\sigma$  actually occur for a strong absorber, these shifts have either to be determined (and corrected) independently, or the DOAS analysis has to be performed by a non-linear algorithm.

## Appendix B

### Discrete derivative

The shift-spectrum involves the first derivative of  $I$ , which has to be calculated numerically. For the comparison of the linear and non-linear fit in Sect. 4, we calculate the derivative as difference quotient:

$$y' = \frac{y(x+h) - y(x)}{h}, \quad (\text{B1})$$

where  $x$  is the pixel number,  $h$  is set to 0.0001 pixel, and  $y(x+h)$  is derived from  $y(x)$  and  $y(x+1)$  by spline interpolation. This approach proves to yield accurate results for the linear fit, particularly for small shifts, but is a rather time-consuming method.

Alternatively, we investigate the fit accuracy for the discrete derivatives

$$y'_0 = \frac{1}{2h}(-y_{-1} + y_1), \quad (\text{B2})$$

## Linearised shift and stretch in DOAS

S. Beirle et al.

Title Page

Abstract

Introduction

Conclusions

References

Tables

Figures

◀

▶

◀

▶

Back

Close

Full Screen / Esc

Printer-friendly Version

Interactive Discussion



and

$$y'_0 = \frac{1}{12h}(y_{-2} - 8y_{-1} + 8y_1 - y_2) \quad (\text{B3})$$

according to Bronstein and Semendjajew (1981) (Sect. 7.1, Table 7.13 therein), where  $h$  is the distance between two  $y$  values. The unit chosen for  $h$  (i.e. 1 pixel or the corresponding wavelength interval) determines the units of the derivative and the fitted shift, respectively.

Table 2 lists the respective fit residues and SCD bias of the different derivative definitions for a shift of 0.002 nm. Compared to the spline-based derivative, both derivatives result in higher residues and SCD bias. However, for the spectra affected by noise, results from the fit using Eq. (B3) are quite close to the spline-based results. Thus we propose to calculate the discrete derivative according to Eq. (B3), which is far faster than the spline-based derivative, but shows far better fit results compared to derivatives based on Eq. (B2).

*Acknowledgements.* We thank Julia Remmers and Kornelia Mies from MPI Mainz for helpful comments on the manuscript. Oliver Woodford is acknowledged for providing the MATLAB routine `export_fig`, which significantly simplifies the processing of MATLAB figures.

The service charges for this open access publication have been covered by the Max Planck Society.

## References

- Boersma, K., Eskes, H., and Brinksma, E.: Error analysis for tropospheric NO<sub>2</sub> retrieval from space, *J. Geophys. Res.*, 109, D04311, doi:10.1029/2003JD003962, 2004. 8383
- Bronstein, I. N. and Semendjajew, K. A.: Taschenbuch der Mathematik, 20th Edn., Verlag Harri Deutsch, Thun, 1981. 8391
- Chance, K. and Kurucz, R. L.: An improved high-resolution solar reference spectrum for Earth's atmosphere measurements in the ultraviolet, visible, and near infrared, *J. Quant. Spectrosc. Ra.*, 111, 1289–1295, doi:10.1016/j.jqsrt.2010.01.036, 2010. 8373, 8380

## Linearised shift and stretch in DOAS

S. Beirle et al.

Title Page

Abstract

Introduction

Conclusions

References

Tables

Figures

◀

▶

◀

▶

Back

Close

Full Screen / Esc

Printer-friendly Version

Interactive Discussion



**Linearised shift and stretch in DOAS**

S. Beirle et al.

Title Page

Abstract

Introduction

Conclusions

References

Tables

Figures

◀

▶

◀

▶

Back

Close

Full Screen / Esc

Printer-friendly Version

Interactive Discussion



- Fayt, C. and van Roozendael, M.: WinDOAS 2.1 Software User Manual, available at: <http://uv-vis.aeronomie.be/software/WinDOAS/WinDOAS-SUM-210b.pdf> (last access: 1 October 2012), 2001. 8374
- Hönninger, G., von Friedeburg, C., and Platt, U.: Multi axis differential optical absorption spectroscopy (MAX-DOAS), *Atmos. Chem. Phys.*, 4, 231–254, doi:10.5194/acp-4-231-2004, 2004. 8374
- Kraus, S.: DOASIS: A framework design for DOAS, Dissertation, University of Mannheim, Germany, 2005. 8374, 8381, 8384
- Marquardt, D. W.: An algorithm for least-squares estimation of nonlinear parameters, *J. Soc. Ind. Appl. Math.*, 11, 431–441, 1963. 8372
- Martin, R.: Satellite remote sensing of surface air quality, *Atmos. Environ.*, 42, 7823–7843, doi:10.1016/j.atmosenv.2008.07.018, 2008. 8374
- Noxon, J. F.: Stratospheric NO<sub>2</sub>, 2: Global behavior, *J. Geophys. Res.*, 84, 5067–5076, doi:10.1029/JC084iC08p05067, 1979. 8371
- 15 Platt, U.: Differential optical absorption spectroscopy (DOAS), in: *Air Monitoring by Spectroscopic Techniques*, Chemical Analysis Series, edited by: Sigrist, M. W., John Wiley, New York, 127 pp., 1994. 8370
- Platt, U. and Stutz, J.: *Differential Optical Absorption Spectroscopy*, Springer-Verlag, Berlin, Heidelberg, 2008. 8370, 8372
- 20 Richter, A. and Wagner, T.: The Use of UV, Visible and Near IR Solar Back Scattered Radiation to Determine Trace Gases, in: *The Remote Sensing of Tropospheric Composition from Space*, edited by: Burrows, J. P., Borrell, P., and Platt, U., Springer, available at: <http://www.springerlink.com/content/x66428846gu0870k/abstract/>, last access: 11 May 2012, Berlin, Heidelberg, 67–121, 2011. 8370
- 25 Rozanov, A., Köhl, S., Doicu, A., McLinden, C., Pukite, J., Bovensmann, H., Burrows, J. P., Deutschmann, T., Dorf, M., Goutail, F., Grunow, K., Hendrick, F., von Hobe, M., Hrechany, S., Lichtenberg, G., Pfeilsticker, K., Pommereau, J. P., Van Roozendael, M., Stroh, F., and Wagner, T.: BrO vertical distributions from SCIAMACHY limb measurements: comparison of algorithms and retrieval results, *Atmos. Meas. Tech.*, 4, 1319–1359, doi:10.5194/amt-4-1319-2011, 2011. 8372, 8376, 8388
- 30



**Linearised shift and stretch in DOAS**

S. Beirle et al.

[Title Page](#)[Abstract](#)[Introduction](#)[Conclusions](#)[References](#)[Tables](#)[Figures](#)[◀](#)[▶](#)[◀](#)[▶](#)[Back](#)[Close](#)[Full Screen / Esc](#)[Printer-friendly Version](#)[Interactive Discussion](#)

Slijkhuis, S., von Bargaen, A., Thomas, W., and Chance, K.: Calculation of under-sampling correction spectra for DOAS spectral fitting, in: ESAMS99 European Symposium on Atmospheric Measurements From Space, Rep. ESA WPP-161, Eur. Space Agency, Noordwijk, The Netherlands, 563–569, 1999. 8371, 8374

5 Solomon, S., Schmeltekopf, A. L., and Sanders, R. W.: On the interpretation of zenith sky absorption measurements, *J. Geophys. Res.*, 92, 8311–8319, doi:10.1029/JD092iD07p08311, 1987. 8371

Stutz, J. and Platt, U.: Numerical analysis and estimation of the statistical error of differential optical absorption spectroscopy measurements with least-squares methods, *Appl. Optics*, 35, 6041–6053, doi:10.1364/AO.35.006041, 1996. 8371

10 Vandaele, A. C., Hermans, C., Simon, P. C., Carleer, M., Colin, R., Fally, S., Mérieu, M. F., Jenouvrier, A., and Coquart, B.: Measurements of the NO<sub>2</sub> absorption cross-section from 42 000 cm<sup>-1</sup> to 10 000 cm<sup>-1</sup> (238–1000 nm) at 220 K and 294 K, *J. Quant. Spectrosc. Ra.*, 59, 171–184, doi:10.1016/S0022-4073(97)00168-4, 1998.

15 Veefkind, J. P., Aben, I., McMullan, K., Forster, H., de Vries, J., Otter, G., Claas, J., Eskes, H. J., de Haan, J. F., Kleipool, Q., van Weele, M., Hasekamp, O., Hoogeveen, R., Landgraf, J., Snel, R., Tol, P., Ingmann, P., Voors, R., Kruizinga, B., Vink, R., Visser, H., and Levelt, P. F.: TROPOMI on the ESA Sentinel-5 precursor: AGMES mission for global observations of the atmospheric composition for climate, air quality and ozone layer applications, *Remote Sens. Environ.*, 120, 70–83, doi:10.1016/j.rse.2011.09.027, 2012. 8372, 8380

20 Wagner, T., Beirle, S., Deutschmann, T., Eigemeier, E., Frankenberg, C., Grzegorski, M., Liu, C., Marbach, T., Platt, U., and de Vries, M. P.: Monitoring of atmospheric trace gases, clouds, aerosols and surface properties from UV/vis/NIR satellite instruments, *J. Opt. A-Pure Appl. Op.*, 10, 104019, doi:10.1088/1464-4258/10/10/104019, 2008. 8374

25 Wagner, T., Beirle, S., Brauers, T., Deutschmann, T., Frieß, U., Hak, C., Halla, J. D., Heue, K. P., Junkermann, W., Li, X., Platt, U., and Pundt-Gruber, I.: Inversion of tropospheric profiles of aerosol extinction and HCHO and NO<sub>2</sub> mixing ratios from MAX-DOAS observations in Milano during the summer of 2003 and comparison with independent data sets, *Atmos. Meas. Tech.*, 4, 2685–2715, doi:10.5194/amt-4-2685-2011, 2011. 8374

30 Williams, G.: Overdetermined systems of linear equations, *Am. Math. Mon.*, 97, 511–513, doi:10.2307/2323837, 1990. 8371

**Linearised shift and stretch in DOAS**

S. Beirle et al.

Title Page

Abstract

Introduction

Conclusions

References

Tables

Figures

⏪

⏩

◀

▶

Back

Close

Full Screen / Esc

Printer-friendly Version

Interactive Discussion

**Table 1.** Variations of shift and stretch applied to the synthetic spectra.

Parameter	Values
Shift (in pixels)	0, $\pm(0.001, 0.003, 0.01, 0.03, 0.1, 0.3, 1)$
Stretch ( $q - 1$ )	0, $\pm(0.00001, 0.0001, 0.001, 0.01, 0.1)$

## Linearised shift and stretch in DOAS

S. Beirle et al.

**Table 2.** Fit residues and NO<sub>2</sub> bias for a shift of 0.002 nm. For the spectra affected to noise, the mean and standard deviation of 300 random spectra is given. All numbers are given with 2 digits, but in fixpoint notation so that the different orders of magnitude are directly visible. The last two fits (5. and 6.) refer to different methods for the calculation of the discrete derivative (see Appendix B).

	Residue [% OD]		NO <sub>2</sub> bias [10 <sup>14</sup> molecules cm <sup>-2</sup> ]	
	w/o noise	with noise	w/o noise	with noise
1. Non-linear	0.00076	(0.095 ± 0.015)	0.0038	(0.2 ± 1.6)
2. Linear	0.33	(0.34 ± 0.026)	3.2	(3.2 ± 1.6)
3. Linear including $A_{\text{Shift/Stretch}}$	0.0011	(0.095 ± 0.015)	0.012	(0.0 ± 1.6)
4. Linear including $B_{\text{Shift/Stretch}}$	0.0045	(0.095 ± 0.015)	0.045	(0.1 ± 1.6)
5. As 3., derivative Eq. (B2)	0.027	(0.10 ± 0.017)	0.48	(0.5 ± 1.7)
6. As 3., derivative Eq. (B3)	0.010	(0.095 ± 0.015)	0.082	(0.1 ± 1.6)

[Title Page](#)
[Abstract](#)
[Introduction](#)
[Conclusions](#)
[References](#)
[Tables](#)
[Figures](#)
[◀](#)
[▶](#)
[◀](#)
[▶](#)
[Back](#)
[Close](#)
[Full Screen / Esc](#)
[Printer-friendly Version](#)
[Interactive Discussion](#)


**Linearised shift and stretch in DOAS**

S. Beirle et al.

Title Page

Abstract

Introduction

Conclusions

References

Tables

Figures

◀

▶

◀

▶

Back

Close

Full Screen / Esc

Printer-friendly Version

Interactive Discussion

**Table 3.** Computation times for linear and non-linear fits from MATLAB and DOASIS in seconds per fit.

	Linear fit	Non-linear fit
MATLAB	$4 \times 10^{-5}$	$5 \times 10^{-2}$
DOASIS	$4 \times 10^{-4}$	$4 \times 10^{-3}$

## Linearised shift and stretch in DOAS

S. Beirle et al.

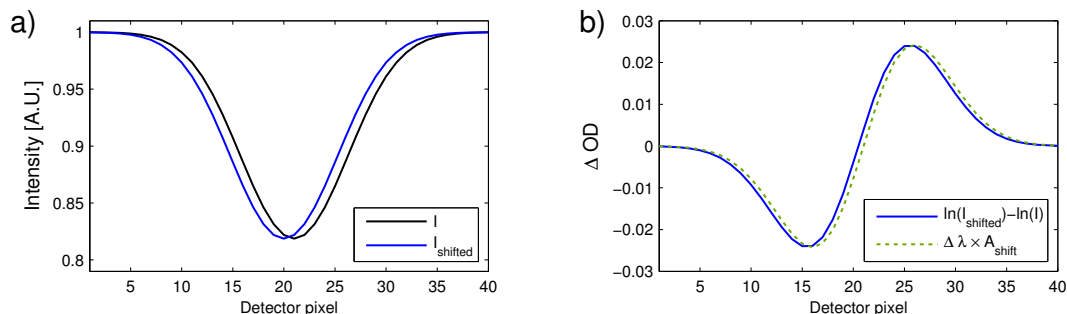


**Fig. 1.** Illustration of the effect of a spectral shift of  $I$ . **(a)** Original (black) and shifted (blue) Intensity  $I$  in artificial units, showing a single absorption line according to Eq. (7), with an optical depth of  $a = 0.2$  and a width  $\zeta$  of 5 pixel, for a shift of  $\Delta\lambda = 1$  pixel. **(b)** Actual difference of the true and shifted OD (blue), compared to the linear approximation, i.e. the pseudo-absorber  $A_{\text{Shift}}$  as defined in Eq. (4), scaled by the applied shift of 1 pixel (green).

Title Page

Abstract

Introduction

Conclusions

References

Tables

Figures

◀

▶

◀

▶

Back

Close

Full Screen / Esc

Printer-friendly Version

Interactive Discussion



## Linearised shift and stretch in DOAS

S. Beirle et al.

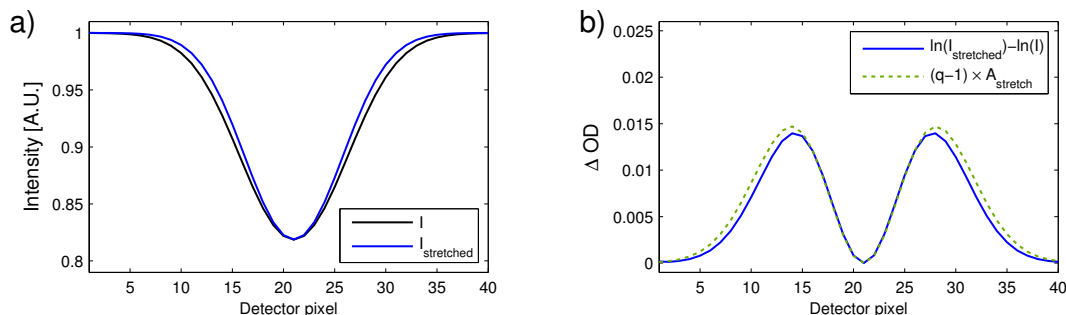


**Fig. 2.** Illustration of the effect of a spectral stretch of  $I$ . **(a)** Original (black) and stretched (blue) Intensity  $I$  in artificial units, showing a single absorption line according to Eq. (7), with an optical depth of  $a = 0.2$  and a width  $\zeta$  of 5 pixel, for a stretch of  $q = 1.1$ . **(b)** Actual difference of the true and stretched OD (blue), compared to the linear approximation, i.e. the pseudo-absorber  $A_{\text{Stretch}}$  as defined in Eq. (15), scaled by the applied stretch  $q - 1$  (green).

Title Page

Abstract

Introduction

Conclusions

References

Tables

Figures

◀

▶

◀

▶

Back

Close

Full Screen / Esc

Printer-friendly Version

Interactive Discussion



## Linearised shift and stretch in DOAS

S. Beirle et al.

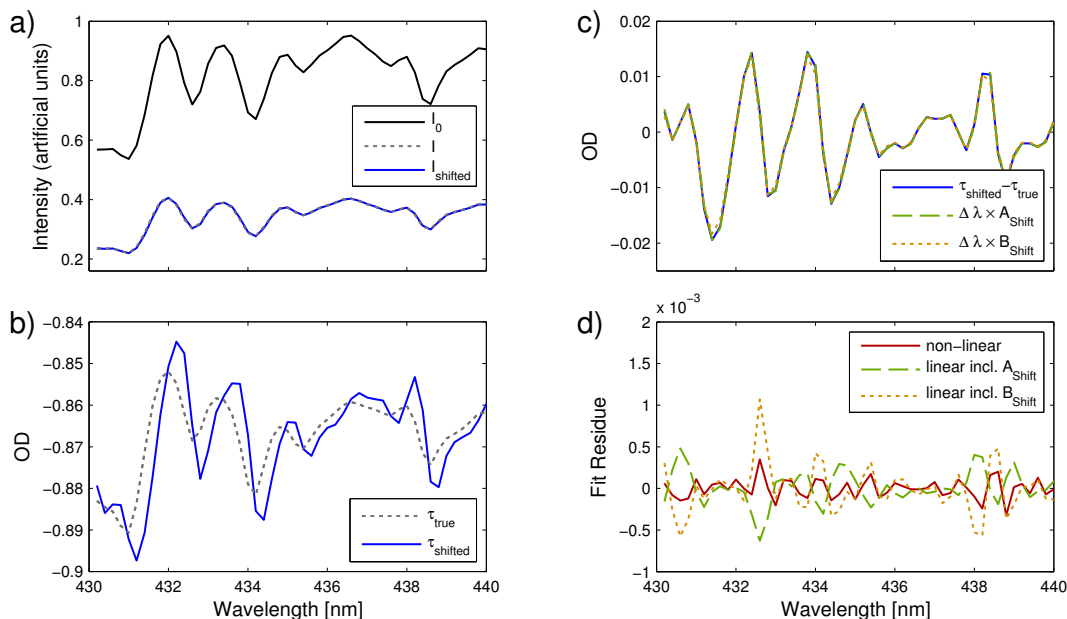


**Fig. 3.** Illustration of the linear and non-linear DOAS fits for a simple synthetic spectrum / including the Ring effect and  $\text{NO}_2$  absorption. **(a)** Intensities  $I_0$ ,  $I$ , and  $I$  shifted by 0.02 nm. **(b)** OD ( $\ln \frac{I}{I_0}$ ) for the original and shifted Intensities. **(c)** Difference of the OD from shifted and original Intensities (blue), and the “shift-spectrum” as defined in Eqs. (4) and (16), scaled by the applied shift of 0.02 nm (green/orange). **(d)** Fit residues for the non-linear fit (red) and the linear fit with shift and stretch pseudo-absorbers included (green/orange).

[Title Page](#)
[Abstract](#)
[Introduction](#)
[Conclusions](#)
[References](#)
[Tables](#)
[Figures](#)
[◀](#)
[▶](#)
[◀](#)
[▶](#)
[Back](#)
[Close](#)
[Full Screen / Esc](#)
[Printer-friendly Version](#)
[Interactive Discussion](#)


## Linearised shift and stretch in DOAS

S. Beirle et al.

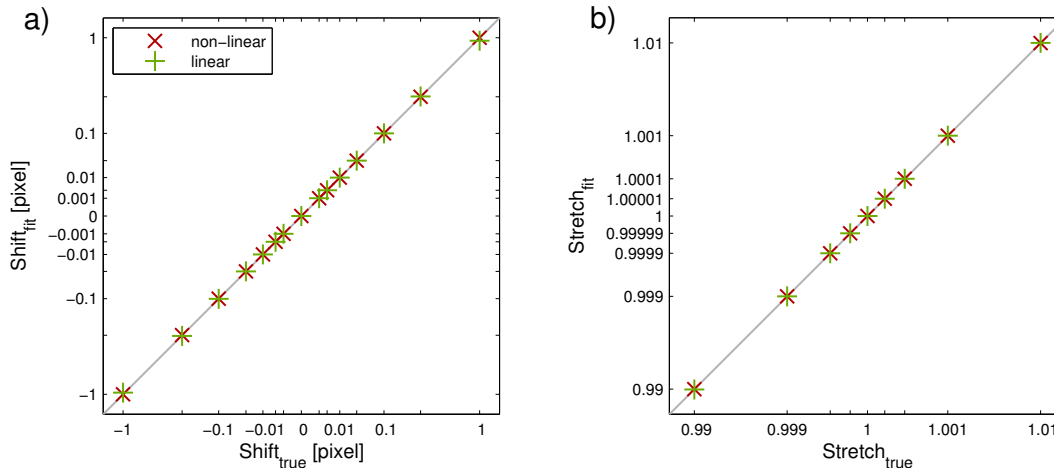


**Fig. 4.** Comparison of the fitted and the true shift (left panel, for stretch  $\equiv$  1) and stretch (right panel, for shift  $\equiv$  0) for the non-linear (red) and the linear fit (green) including  $A_{\text{Shift}}$  and  $A_{\text{Stretch}}$ , respectively. The applied shifts and stretches are listed in Table 1. The grey line shows 1 : 1 correspondence. Note that the scales are nonlinear to show the full range of variations over some orders of magnitude.

Title Page

Abstract

Introduction

Conclusions

References

Tables

Figures

◀

▶

◀

▶

Back

Close

Full Screen / Esc

Printer-friendly Version

Interactive Discussion





## Linearised shift and stretch in DOAS

S. Beirle et al.

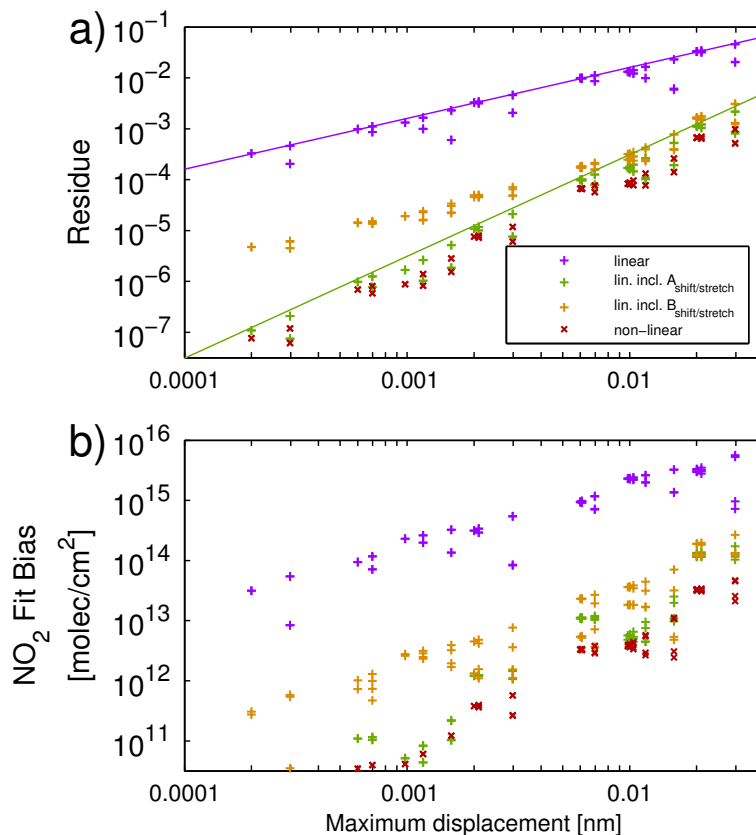


**Fig. 5.** Dependency of the peak-to-peak fit residue (a) and the absolute  $\text{NO}_2$  bias (b) on the maximum spectral displacement caused by the combined shifts and stretches applied, for the non-linear and various linear fits, on a log-log-scale. The purple and green lines indicate the estimated first- and second order effects of a spectral displacement, according to Eqs. (9) and (12), for  $a = 0.4$  and  $\zeta = 0.3$  nm.

**Linearised shift and stretch in DOAS**

S. Beirle et al.

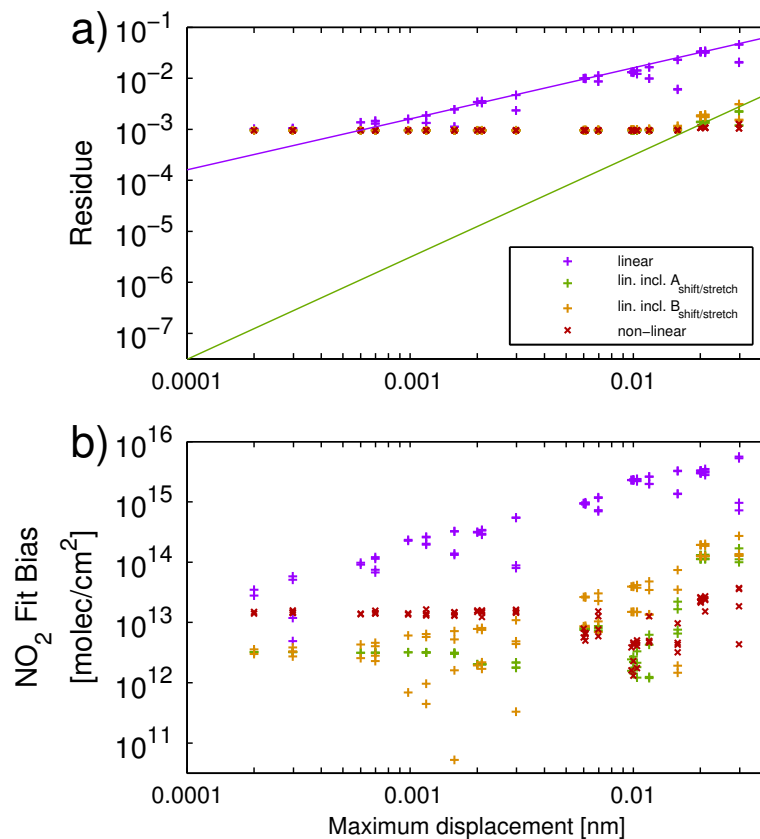


**Fig. 6.** As Fig. 5 for synthetic radiances with additional Gaussian noise of 0.015 %.

Title Page

Abstract

Introduction

Conclusions

References

Tables

Figures

◀

▶

◀

▶

Back

Close

Full Screen / Esc

Printer-friendly Version

Interactive Discussion



## Linearised shift and stretch in DOAS

S. Beirle et al.

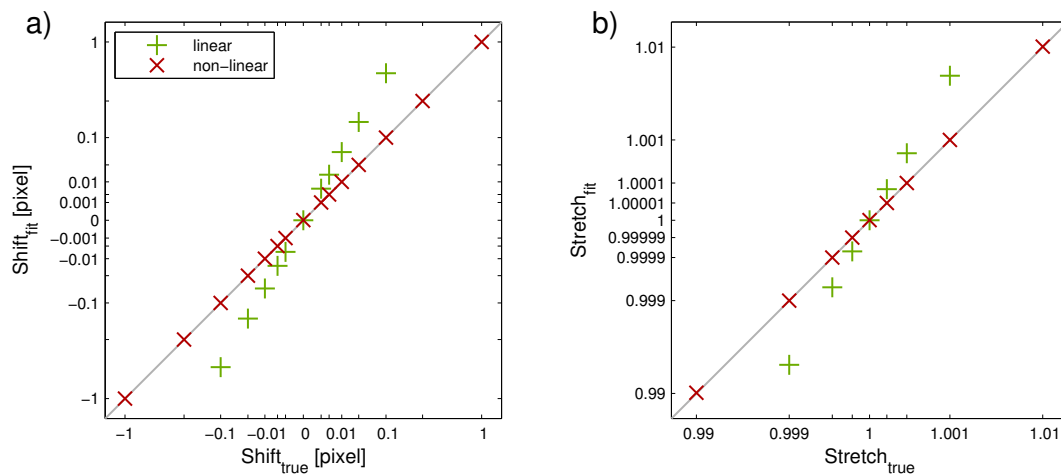


**Fig. A1.** As Fig. 4, but for shifts in the absorption cross-section of NO<sub>2</sub>. The fitted shifts/stretch for  $A_{\text{Shift}}^{\sigma}$  and  $A_{\text{Stretch}}^{\sigma}$  are off by almost an order of magnitude due to the remaining non-linearities (see text).